

Cooperative cavitation in rubber-toughened polycarbonate

C. CHENG, A. HILTNER*, E. BAER

Department of Macromolecular Science, and Center for Applied Polymer Research, Case Western Reserve University, Cleveland, OH 44106, USA

P. R. SOSKEY, S. G. MYLONAKIS

EniChem America Inc., Research and Development Center, 2000 Cornwall Road, Monmouth Junction, NJ 08852, USA

Particle cavitation in the stress-whitened zone ahead of a semicircular notch in polycarbonate blended with a core-shell rubber was characterized by transmission electron microscopy. Cavitation of rubber particles at five locations in the stress-whitened zone was correlated with the local stress and strain history. It was found that cavitation initiated some distance ahead of the notch when a mean stress condition was met. Initially, only a fraction of the particles cavitated and these were randomly distributed. Single cavitated particles grew into cavitated domains by cooperative cavitation of nearby particles until cavitation was arrested when shear yielding of the matrix provided an alternative mechanism for relief of strain energy. Far from the notch, where the stress state approached uniaxial tension, cavitated domains grew into linear arrays of cavitated particles. A mechanism of cooperative crazing in microlayer composites of polycarbonate and styrene/acrylonitrile copolymer was adapted to cooperative cavitation of core-shell rubber particles. It was proposed that cooperative cavitation of nearby particles occurred by impingement of a small plastic zone that formed at the equator of a cavitated particle.

1. Introduction

Cooperative cavitation of core-shell rubber particles in blends with polycarbonate may impart higher impact strength, especially at low temperatures, by facilitating cavitation and promoting matrix shear. We observed linear arrays of cooperatively cavitated rubber particles in the stress-whitened regions of blends with particle concentrations of 5% or more [1]. The arrays were found in the damage zone that accompanies the fracture surface of -20°C Izod impacts, and also in the stress-whitened zone that forms ahead of a semicircular notch during slow tensile loading. Cooperative cavitation is not unique to polycarbonate blends. Linear arrays of cavitated core-shell rubber particles are reported in toughened epoxies [2, 3].

The semicircular notch geometry is especially useful when the objective is to characterize evolution of prefracture deformation under a known stress state [4]. To understand the sequence of events that leads to cavitated arrays, the particle morphology in a polycarbonate blend was examined at various positions through the damage zone ahead of a semicircular notch. Comparisons were made with microlayer composites of polycarbonate and styrene-acrylonitrile copolymer, a "one-dimensional" model system that also exhibits cooperative cavitation [5, 6]. By

considering the local stress state at a cavitated particle, it was possible to propose a mechanism for cooperative cavitation of rubber particles in a ductile matrix.

2. Materials and methods

The matrix polymer was a commercial polycarbonate (PC), produced by EniChem SpA, designated as Sinvet 251, with a molecular weight of about 32 000. The MBS impact modifier was Paraloid EXL-3607 (PL) from Rohm and Haas Co. The monodisperse PL particles were $0.2\ \mu\text{m}$ in diameter.

The starting materials were extruded as described previously and injection moulded into ASTM D638 dogbone-shaped specimens, 3.14 mm thick [1, 4]. A 1 mm radius semicircular notch was machined with an end mill midway along one edge of the tensile specimens. Alternatively, a circular hole with a 1 mm radius was machined in the centre of the gauge section midway between the edges. The notched specimens were mounted in an Instron machine with 115 mm separating the grips, and were loaded at a crosshead speed of $0.1\ \text{mm min}^{-1}$ at ambient temperature.

A $300\ \mu\text{m}$ thick section was cut from the midplane of the damage zone with an Isomet diamond saw. Sections for transmission electron microscopy (TEM) were prepared as described previously [1] by

* Author to whom all correspondence should be addressed.

embedding the 300 μm thick section in epoxy resin, Hysol RE-2038 from Dexter, which cured in 8 h at ambient temperature. The block was carefully trimmed with a glass knife, with the assistance of an optical microscope operated in the reflection mode, to expose the desired region of the damage zone. The block was then stained by immersion for 3 days in a 2% aqueous solution of osmium tetroxide, thin sections were wet cryo-microtomed with a diamond blade in an RMC MT6000-XL ultramicrotome equipped with a CR-2000 cryosectioning unit. The 90–120 nm sections were examined in a Jeol 100SX transmission electron microscope.

3. Results and discussion

3.1. Macroscale deformation zone at a semicircular notch

The stress displacement curve of polycarbonate with 10% PL is shown in Fig. 1a. The deformation zone ahead of the semicircular edge notch was examined by sectioning the opaque specimen after it was loaded. The sketch in Fig. 1b of the growth of the deformation zone during tensile loading is based on results published previously [1, 4]. Yielding in the centre of the specimen at the notch root began when the remote stress reached about 60% of the tensile yield stress ($0.6\sigma_T$). The yielded region, designated as the core yielding zone (CYZ), consisted of two sets of fine slip lines that grew out from the notch root. At a slightly higher stress, S_1 , a dark region appeared at the tip of the core yielding zone. The darkness was caused by light scattering from cavitated rubber particles, and therefore this region was designated as the stress-whitened zone (SWZ). The circular shape of the SWZ

when it first appeared gradually changed to triangular as the SWZ increased in size with increasing remote stress. Because the CYZ also continued to increase in size as the stress increased, the CYZ always overlapped part of the SWZ. The critical condition for cavitation was determined from the position of the near notch boundary of the SWZ relative to the notch root [4]. Because the critical condition did not depend on the rubber content of the blend, it appeared that initiation of cavitation was not affected by interparticle separation. The critical cavitation condition did, however, change from one rubber to another, which meant that this parameter could be used to assess and compare cavitation resistance of various rubber impact modifiers.

The schematic representation of the mean stress distribution in Fig. 2 describes the condition for stress-whitening after core yielding has initiated at the notch root [7]. The mean stress in the CYZ increases away from the notch root to a maximum at the tip. The tip indicates the position of the plastic–elastic boundary; further from the notch root the decreasing mean stress follows a redistributed elastic curve. The stresses in the CYZ are calculated from slip-line theory [8]. The principal stresses σ_1 and σ_2 along the x -axis are given by

$$\begin{aligned}\sigma_y &= \sigma_1 \\ &= \frac{2}{3^{1/2}} \sigma_T [1 + \ln(r/a)]\end{aligned}\quad (1)$$

$$\begin{aligned}\sigma_x &= \sigma_2 \\ &= \frac{2}{3^{1/2}} \sigma_T [\ln(r/a)]\end{aligned}\quad (2)$$

and for the fully plane strain condition

$$\begin{aligned}\sigma_z &= \sigma_3 \\ &= 0.5(\sigma_1 + \sigma_2) \\ &= \frac{2}{3^{1/2}} \sigma_T [0.5 + \ln(r/a)]\end{aligned}\quad (3)$$

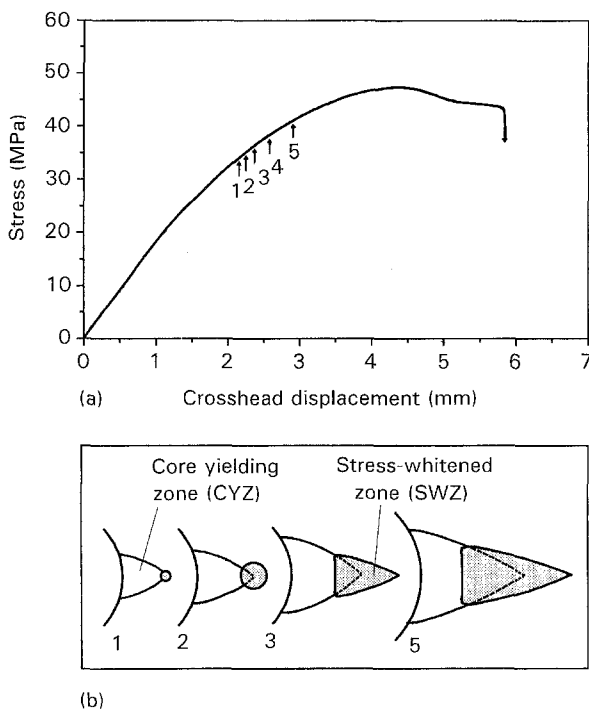


Figure 1 Deformation of semicircular notched PC blend with 10% PL. (a) The stress-displacement curve; and (b) the deformation zone.

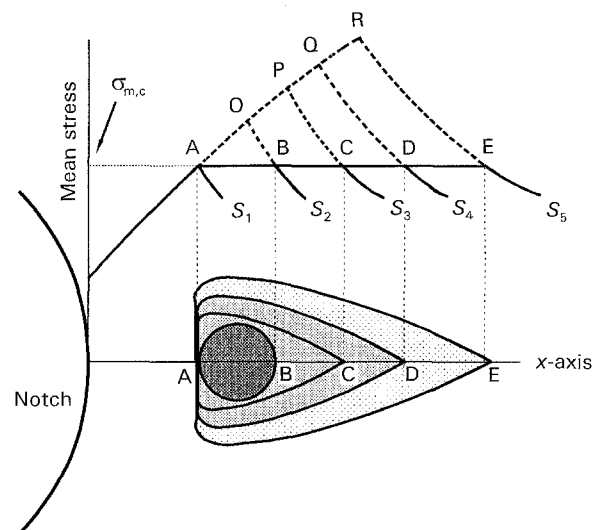


Figure 2 Mean stress distribution ahead of semicircular notch during growth of the deformation zone.

where σ_T is the tensile yield stress of the blend, a is the notch radius and r is the distance from the tip of the core yielding zone to the notch origin. It is apparent from the slip-line equations that the principal stresses in the CYZ increase away from the notch root in a manner that depends on the distance from the notch root, but not on the remote stress. With increasing remote stress, the tip of the CYZ moves outward from the notch root, and the stresses at the tip increase accordingly. Cavitation initiates when the CYZ has grown to position A at S_1 where the mean stress $\sigma_m = (\sigma_1 + \sigma_2 + \sigma_3)/3$ at the tip is equal to the critical mean stress for cavitation, $\sigma_{m,c}$. As the remote stress increases from S_1 to S_5 , the tip of the CYZ moves from position A to position R. The region where the mean stress is higher than $\sigma_{m,c}$ corresponds to the SWZ. The dashed lines in Fig. 2 refer to the plane strain condition. When the local triaxial stress ahead of the semicircular notch exceeds the critical value, cavitation of rubber particles in the blend relieves the triaxiality and enables the PC matrix in the SWZ to deform in shear [9]. Because the stress is relieved by cavitation, the mean stress in the SWZ is essentially constant and equal to the critical mean stress, the solid line in Fig. 2. If it is assumed that cavitation relieves specifically σ_3 , the stress state gradually changes from almost plane strain at the near notch boundary of the SWZ to close to plane stress at the far notch boundary.

3.2. Particle cavitation in the stress-whitened zone

The particle morphology was examined at five positions in the SWZ of specimens that were loaded to S_5 ($0.8\sigma_T$). The near notch boundary of the SWZ was located about 0.35 mm from the notch root and, at this remote stress, the far notch boundary was about 1.0 mm from the notch root. Slip-line theory predicted the tip of the CYZ to be about 0.6 mm from the notch root. Sections were microtomed from five positions (X_1 to X_5) located approximately 0.40, 0.45, 0.60, 0.75 and 1.00 mm from the notch root. For convenience, the SWZ was divided into two regions: the near notch region which extended from the near notch boundary of the SWZ to the tip of the CYZ, and the far notch region which extended from the tip of the CYZ to the far notch boundary of the SWZ. Positions X_1 and X_2 were in the near notch region, position X_3 coincided with the plastic-elastic boundary at the tip of the CYZ, and positions X_4 and X_5 were in the far notch region.

The mean stress in the region of the CYZ between the notch root and the SWZ was below the critical cavitation stress. Rubber particles in this region were not cavitated or otherwise deformed. The morphology was indistinguishable from that of the undeformed blend where the particles were distributed as isolated particles, or as small clumps or strings of two to ten particles, Fig. 3a. The micrograph of a section from position X_1 in the SWZ contained primarily single cavitated particles, these could either be isolated or

could be in a clump with uncavitated particles, Fig. 3b. The micrograph also shows clumps where most of the particles were cavitated. More particles were cavitated at position X_2 than at X_1 , Fig. 3c. In addition to single cavitated particles and small clumps of cavitated particles, there were regions where eight or more cavitated particles formed an elongated array oriented perpendicular to the loading direction. The fraction of particles that were cavitated increased further at positions X_3 and X_4 , Fig. 3d and e. The number and length of the cavitated arrays also increased at these positions while the number of isolated cavitated particles and small clumps of cavitated particles decreased. At the tip of the SWZ, position X_5 , particle cavitation resembled that at position X_1 with single cavitated particles and small clumps of cavitated particles, Fig. 3f.

The TEM observations are summarized in Fig. 4. In general, cavitation was observed as single cavitated particles, small clumps of cavitated particles, and linear arrays of cavitated particles. The distribution of cavitated particles among the three types of domains varied from one position in the SWZ to another. Single cavitated particles and small clumps dominated at positions X_1 and X_5 , no cavitated arrays were seen at these positions. In contrast, although some single cavitated particles and small clumps were observed at all positions in the SWZ, most of the cavitated particles at positions X_3 and X_4 were in arrays. In low-magnification electron micrographs, the arrays at positions X_2 , X_3 and X_4 appeared as parallel dark, wavy bands oriented approximately perpendicular to the loading direction. They corresponded closely in orientation and size to irregular wavy lines that characterized the microscale texture in optical micrographs of the far notch region [1]. At higher magnification, they consisted of thin rows of cavitated particles with a broad range in length; they typically incorporated one to four cavitated particles in the width and from 8–35 cavitated particles in the length. Sometimes distortion of the cavitated particles in the array suggested that locally the matrix was highly deformed. The three-dimensional shape of the cavitated arrays was obtained by comparing sections from the three orthogonal planes. The three views were combined to reveal disc-shaped cavitated domains with the plane of the disc oriented perpendicular to the loading direction [1].

The number fraction of cavitated particles was determined from the micrographs, and is plotted in Fig. 5 as a function of position in the deformation zone. Only area features are reported, although previous reconstructions of volume parameters from area features indicated that the actual values might be somewhat larger [1]. In the near notch region of the SWZ, the cavitated particle fraction increased from 0 at the near notch boundary to 0.13 at position X_1 , 0.18 at position X_2 and 0.35 at X_3 , the tip of the CYZ. Position X_4 , which was located outside the CYZ in the far notch region, had the same fraction of cavitated particles, 0.35, as position X_3 . At the far notch tip of the SWZ, position X_5 , the cavitated particle fraction decreased again to 0.09.

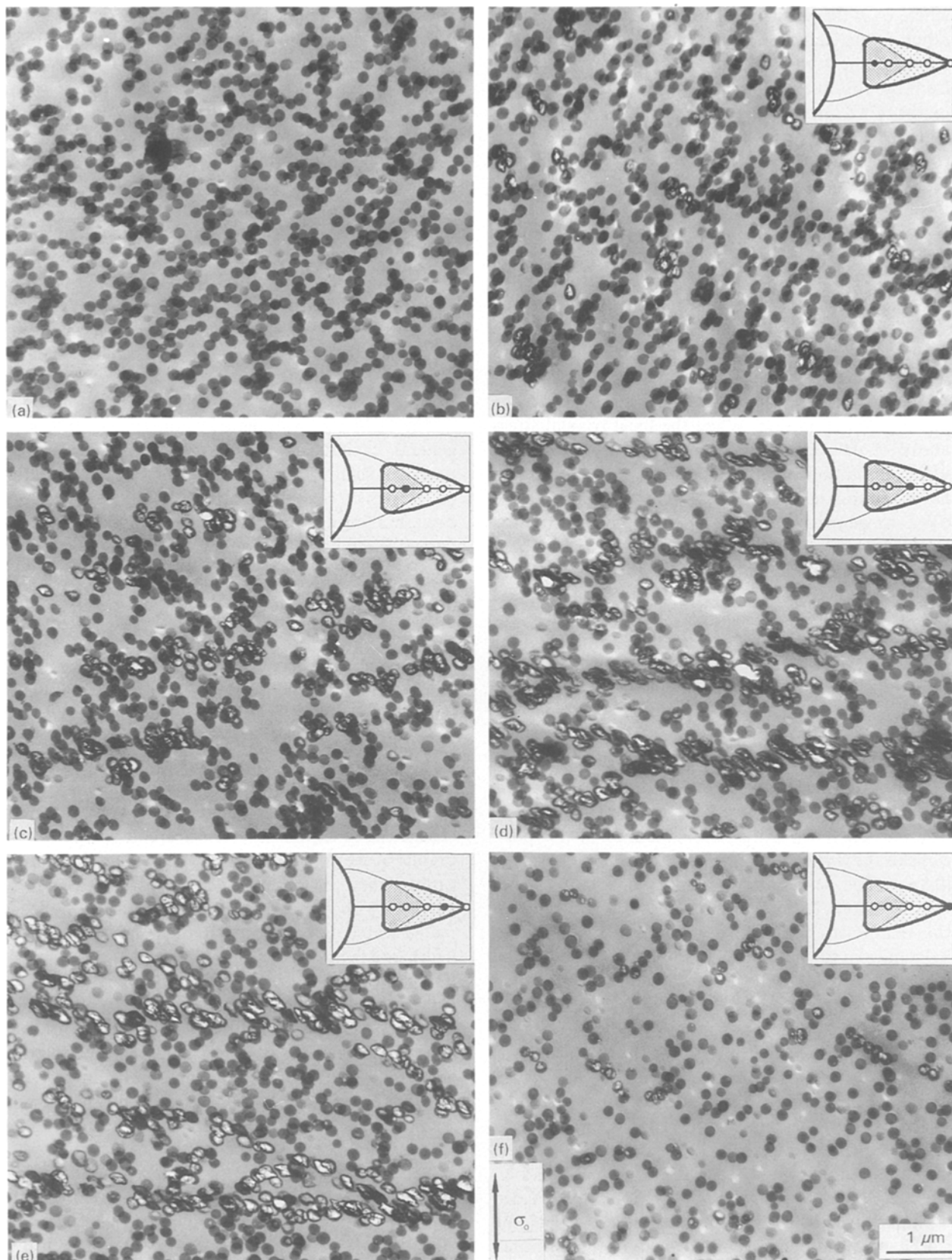


Figure 3 Transmission electron micrographs of sections from the 10% PL blend. (a) The undeformed blend; (b–f) loaded to a remote stress S_5 and sectioned (b) 0.40 mm (X_1), (c) 0.45 mm (X_2), (d) 0.60 mm (X_3), (e) 0.75 mm (X_4) and (f) 1.00 mm (X_5) from the notch root. The loading direction was vertical.

The cavitated particles were distributed among the three types of domains defined in Fig. 6: single cavitated particles, small clumps with two to eight cavitated particles, and arrays with more than eight

cavitated particles. Because there was not much variation in the thickness of arrays, a general correlation existed between the number of cavitated particles in an array and the length of the array. The increase in

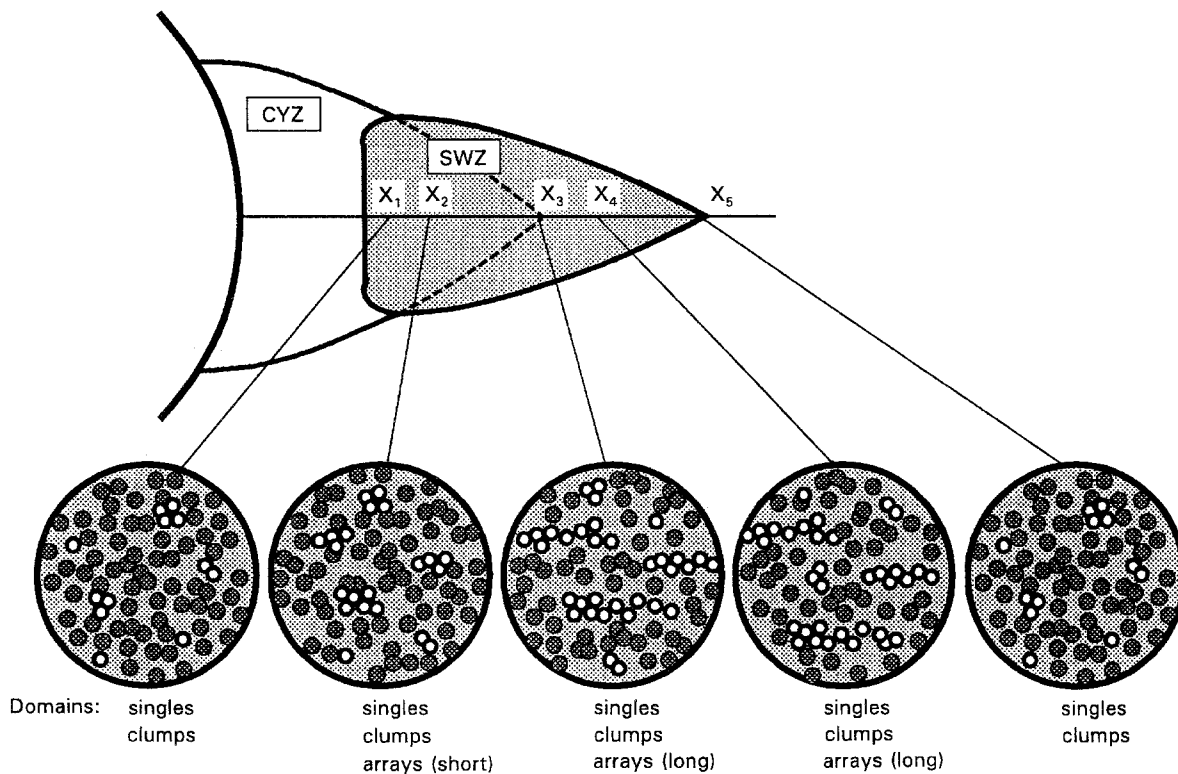


Figure 4 Schematic representation of the particle morphology at various locations in the stress-whitened zone at a remote stress S_5 .

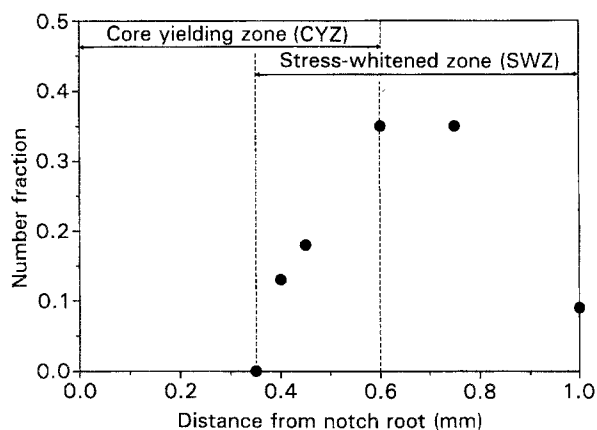
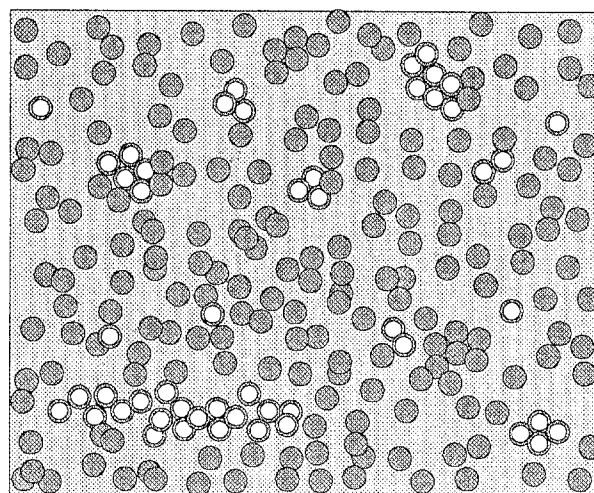


Figure 5 Number fraction of cavitated particles as a function of position in the deformation zone at a remote stress S_5 .

the number of cavitated particles between positions X_1 and X_3 was accompanied by a trend toward larger domains in the form of longer arrays.

The distribution of domain sizes is plotted in Fig. 7 as the cumulative number of cavitated domains per $100 \mu\text{m}^2$. The domains at position X_1 consisted predominantly of single cavitated particles with some small clumps incorporating up to eight cavitated particles. With increasing distance from the notch root, the population of single cavitated particles and clumps decreased while the number of arrays increased. The largest arrays at position X_2 contained 15 cavitated particles, this number increased to 20 particles at positions X_3 and X_4 . The total number of cavitated domains at each position is included in Table I together with the fraction of cavitated particles and the type of domains observed. Despite large differences from one position to the next in the fraction of




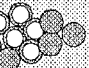
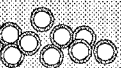
	Number of cavitated particles in domains	Shape
	1	Single
	2 - 8	Clump
	8 - 20	Array

Figure 6 Definition of the three types of cavitated domains.

cavitated particles and the size of cavitated domains, the density of cavitated domains remained approximately constant with about 67 cavitated domains per $100 \mu\text{m}^2$.

3.3. Evolution of cavitated arrays

It was possible to infer a sequence of cavitated domain initiation, growth and arrest from the constant density of cavitated domains and the consequent relationship between cavitated particle fraction and domain size. It was proposed that during the initiation phase, random cavitation produced single cavitated particles. Initiation was followed by a growth phase when cooperative cavitation of nearby particles caused single cavitated particles to grow into clumps and arrays. Initiation of new domains by random cavitation was negligible during this phase. Initiation and growth of cavitated domains was arrested when shear deformation of the matrix provided an alternative mechanism for relief of strain energy. This occurred in the near notch region when the CYZ grew into the SWZ, and accounted for the smaller domains and lower fraction of cavitated particles at positions X_1 and X_2 compared to positions X_3 and X_4 . Position X_5 at the far notch boundary of the SWZ was representative of the initiation phase.

The deformation zone at a semicircular notch would have evolved during tensile loading as shown in Fig. 8. The remote stress required to meet the yield condition at the notch root was lower than that required to meet the cavitation condition, and the initial irreversible deformation was shear yielding at the notch root in the form of core yielding. As long as the remote stress was less than S_1 , the mean stress everywhere ahead of the notch was less than the critical mean stress for cavitation and only shear yielding at the notch root was observed. At a remote stress S_1 , the cavitation condition was reached at the tip of the

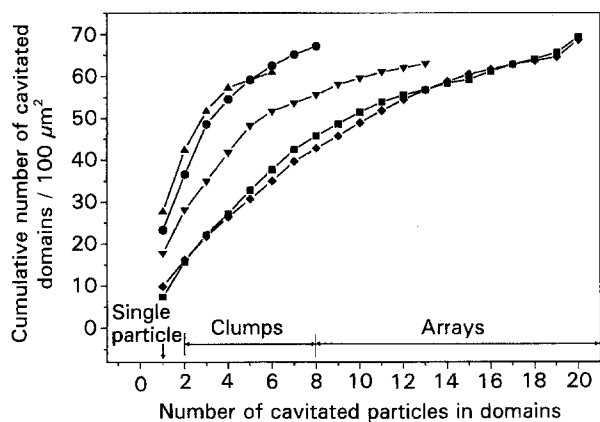


Figure 7 Cumulative number of cavitated domains at five positions X_1 – X_5 in the stress-whitened zone at a remote stress S_5 . (●) X_1 , (▼) X_2 , (■) X_3 , (◆) X_4 , (▲) X_5 .

lengthening CYZ. Cavitation initiated at position X_1 in the unyielded material just ahead of the CYZ. When the stress increased to S_2 , the CYZ overtook position X_1 and cavitation at this position ceased approximately at the end of the initiation phase. Thus only small cavitated domains were observed at this position. Also at S_2 , cavitation initiated at position X_2 some distance ahead of the CYZ. In general, as the remote stress increased, cavitation initiated further ahead of the CYZ and continued further into the growth phase before being arrested by the CYZ. Thus cavitation initiated at position X_3 when the stress was S_3 and the cavitated domains continued to grow until the CYZ reached position X_3 at a stress S_5 . Before being arrested, the domains at X_3 had grown much larger than at either position X_1 or X_2 . At S_5 , the cavitated domains at position X_4 remained in the growth phase. Near the tip of the SWZ at position X_5 , cavitation was in the initiation phase as indicated by the small number of cavitated domains, most of which were single cavitated particles.

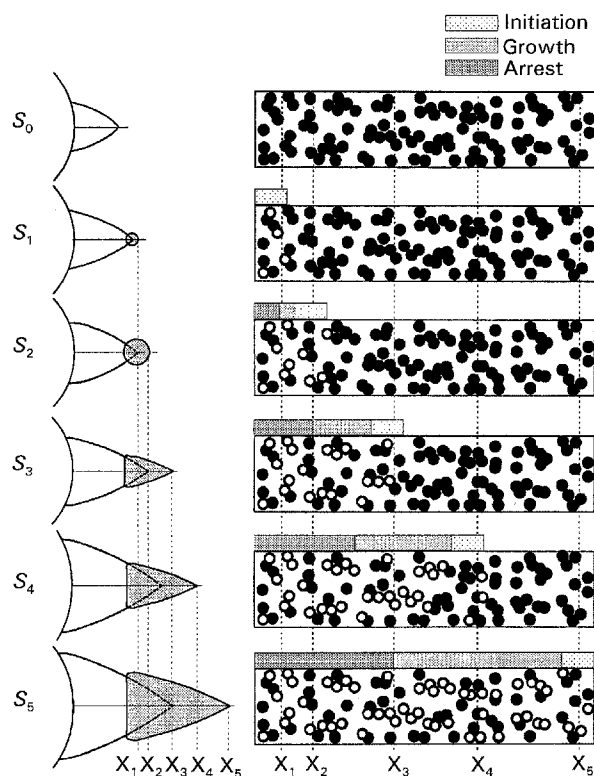


Figure 8 Schematic representation showing evolution of the macroscale deformation zone in polycarbonate with 10% PL and the accompanying nanoscale particle cavitation.

TABLE I Comparison of cavitation features at different locations in the stress-whitened zone

	Position				
	X_1	X_2	X_3	X_4	X_5
Fraction of particles cavitated	0.13	0.18	0.35	0.35	0.09
Number of cavitated domains/ $100 \mu\text{m}^2$	67	63	69	69	60
Types of cavitated domains	Singles, clumps	Singles, clumps, arrays(short)	Singles, clumps, arrays(long)	Singles, clumps, arrays(long)	Singles, clumps

3.4. Mechanism of cavitated array formation

A macromechanics approach has proved valuable for understanding certain aspects of particle cavitation in polymer blends. Specifically, the critical cavitation condition [4] and the subsequent effect of particle cavitation on matrix shear yielding [10] are features of blend behaviour that are amenable to macroscale analysis. Interactive phenomena at the size scale of the particles, such as cooperative cavitation, may be more appropriately addressed by consideration of the local micromechanics. A high magnification micrograph of some arrays of cavitated rubber particles in a polycarbonate blend is compared in Fig. 9 with arrays of crazes in a microlayer composite composed of alternating layers of PC and SAN. Both cavitated arrays in the blend and craze arrays in the microlayer are made up of many aligned voids separated by PC ligaments. The arrays in both instances propagate over a large distance with many cavitation events. Both phenomena require the separation of voiding elements to be less than a critical value. When the microlayer is deformed in uniaxial tension, craze arrays form only if the thickness of the PC layers in between SAN layers is less than $1.2\ \mu\text{m}$ [5, 6].

Cooperative crazing of SAN microlayers is caused by the plastic zone that forms in the PC layer at the

SAN craze tip. When the PC layer thickness is comparable to the length of the plastic zone, the plastic zone impinges on the interface with the neighbouring SAN layer and initiates a craze. The result of repeated impingements is a craze array with many aligned crazes in neighbouring SAN layers. Cooperative crazing in response to a local elastic stress concentration is also identified in the model microlayers when the PC layers are too thick for the plastic zone to impinge on the next SAN layer, but still thin enough that the elastic stress concentration from the plastic zone increases the probability of crazing in the neighbouring SAN layer. In both experimental observations and model calculations, the elastic stress intensification can account for arrays with two or three aligned crazes, but not for arrays with many aligned crazes.

Cooperative cavitation of rubber particles in polymer blends is often discussed with reference to interacting local elastic stress fields [11], and this may be the explanation for arrays of cavitated particles in some brittle matrices [3]. Hitherto, the possibility of shear yielding at the cavitated particle with formation of a small plastic zone has not been considered. A mechanism similar to that of craze array formation in microlayers may be responsible for arrays of cavitated rubber particles in ductile matrix polymers such as polycarbonate. Although the macroscale volume change from particle cavitation may be negligibly small, individual particles may experience a significant increase in volume when they cavitate. Volume dimensions reconstructed from features measured in the micrographs included an increase in the diameter of cavitated particles from $0.18\ \mu\text{m}$ to $0.21\ \mu\text{m}$ [1]. In a balanced triaxial stress state, this volume change might not produce local yielding of the matrix. However, it is suggested that cavitation of the particle in response to the local mean stress relieves σ_3 and also σ_2 locally so that σ_1 is much larger than either σ_3 or σ_2 . Under the local principal stress imbalance, the yield condition is achieved at the equator and a small plastic zone forms in the PC matrix. If a neighbouring particle is close enough that the length of the plastic zone is comparable to the interparticle distance, impingement of the plastic zone can induce it to cavitate.

To estimate the size of the plastic zone, it is assumed that a particle is transformed by the process of cavitation from a load-bearing rubber sphere of diameter $0.18\ \mu\text{m}$ to a hole of diameter $0.21\ \mu\text{m}$. Because core yielding of PC is described by slip line analysis without reference to size scale, it is possible to estimate the relationship between the increase in hole size and length of the plastic zone from measurements on a size scale several orders of magnitude larger. For this purpose, PC with a 2 mm diameter circular hole was loaded uniaxially and the length of the CYZ, L_p , was determined as a function of the hole opening, D . The linear relationship between the hole opening and the length of the CYZ in Fig. 10 was obtained. The arrow in Fig. 10 indicates the relative opening for a cavitated rubber particle that increases in diameter from $0.18\ \mu\text{m}$ to $0.21\ \mu\text{m}$. Assuming that a spherical hole and a circular hole produce a comparable CYZ, the

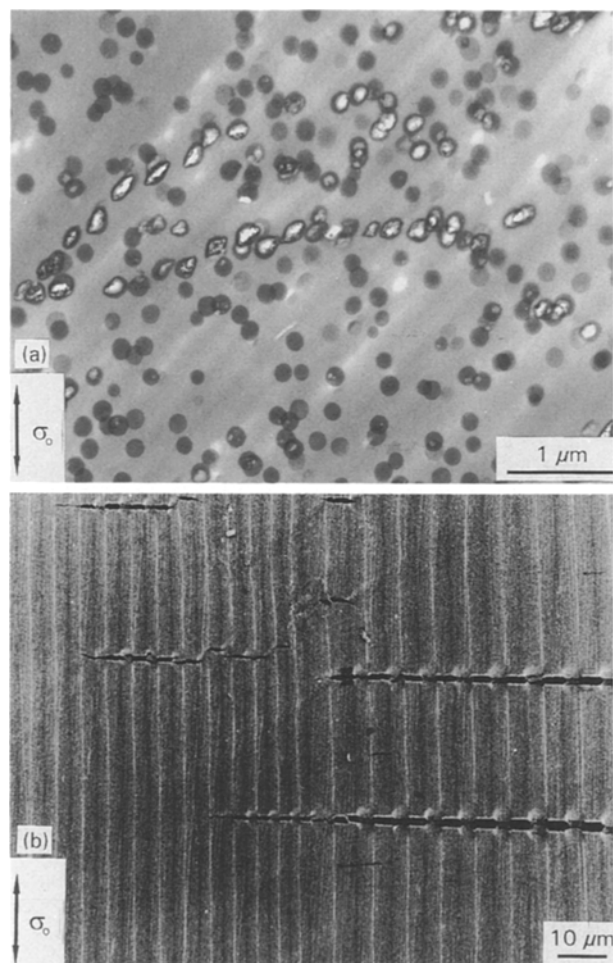


Figure 9 Micrographs of cooperative cavitation. (a) Cavitated arrays of core-shell rubber particles in a PC blend with 5% PL; and (b) craze arrays in a PC/SAN microlayer composite.

length of the small plastic zone formed at a cavitated rubber particle is estimated to be 0.06 μm .

Cavitated arrays in the polycarbonate blend with 10% PL typically form from strings of particles. The particle separation in these strings is of the order of 0.05 μm , consistent with the estimated length of the plastic zone. Formation of a cavitated array from a string of particles is illustrated in Fig. 11. The initial event is cavitation of a single particle in response to the local mean stress field. Cavitation alters the local stress state, and the increased size of the particle is accommodated by formation of a small plastic zone in the matrix. The plastic zone impinges on the neighbouring particle and induces it to cavitate. The process is repeated as the plastic zone from the newly cavitated particle impinges on the next particle. Strings of particles become shorter and less numerous as the amount of PL in the blend decreases to the point that none are observed in the blend with 2% PL

[1]. Correspondingly, the longest cavitated arrays are seen in the 10% PL blend, shorter arrays in the 5% PL blend, and no arrays are seen in the SWZ of the blend with 2% P, Fig. 12.

Cooperative cavitation of rubber particles followed by extension of the PC ligaments between cavitated particles leads to large local strains. If the PC ligaments do not fracture, large macroscopic strains are possible by deformation of the material between arrays until the matrix is uniformly extended.

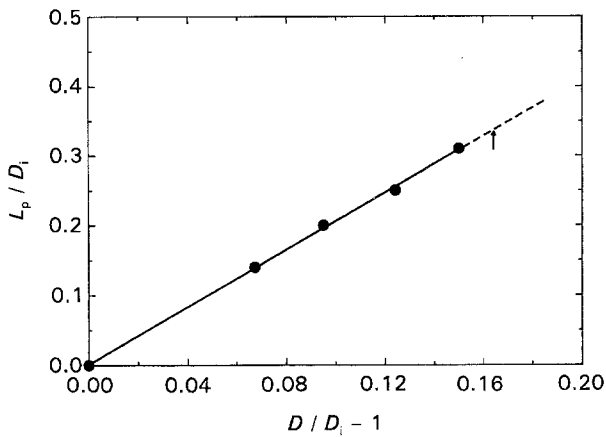


Figure 10 The length of the core yielding zone at a circular hole as a function of the hole opening in polycarbonate: L_p is the length of the core yielding zone, D_i is the initial hole diameter equal to 2 mm, and D is the hole diameter in uniaxial tension. The arrow indicates the relative opening for a cavitated rubber particle that increases in diameter from 0.18 μm to 0.21 μm .

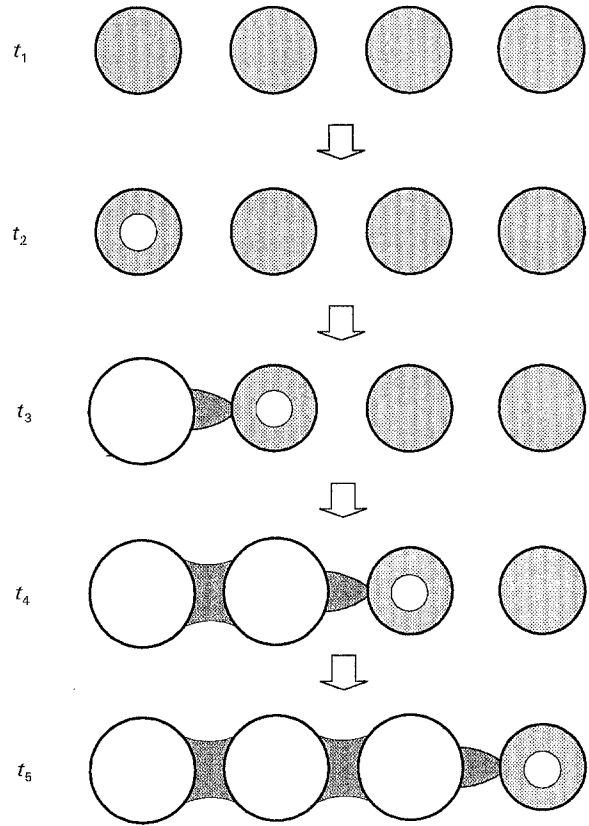


Figure 11 Schematic representation of cavitated arrays formation by plastic zone impingement.

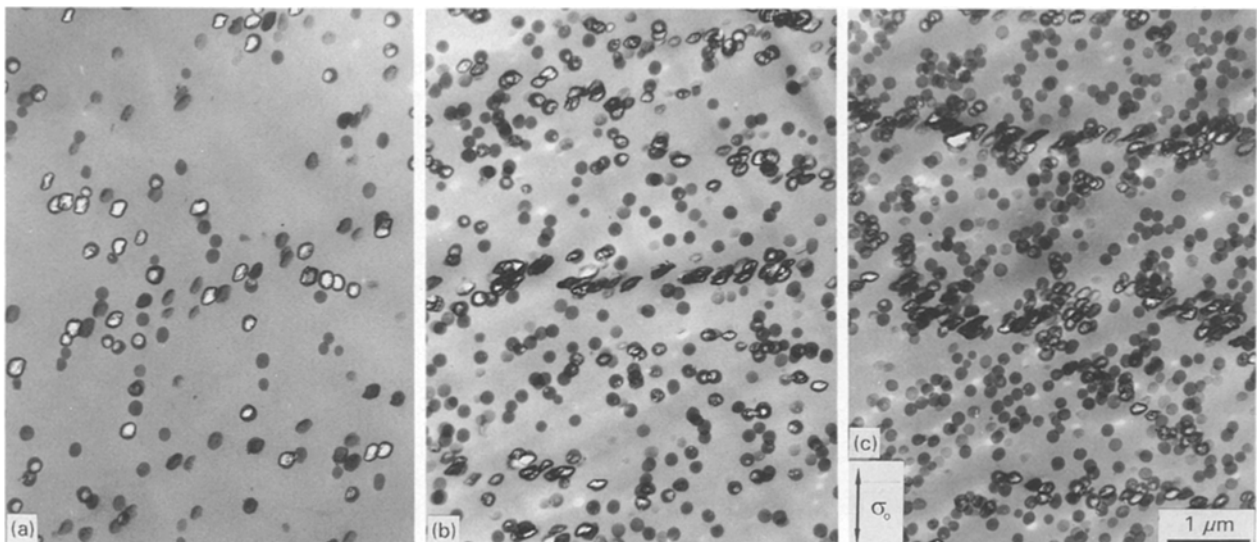


Figure 12 Transmission electron micrographs of sections from the far notch region of the stress-whitened zone. (a) Polycarbonate blend with 2% PL; (b) with 5% PL; and (c) with 10% PL.

Cooperative cavitation may have implications for the impact strength of blends with higher concentrations of rubber particles. The possibility that particle-particle interactions facilitate cavitation and promote matrix shear is especially relevant to low-temperature impact strength. Cavitation arrays have been observed in the damage zone of -20°C impact specimens, where they appear to be a transitional phase between random cavitation of isolated particles and complete cavitation of all the particles [1].

4. Conclusions

Particle cavitation in the stress-whitened zone ahead of a semicircular notch in polycarbonate blended with a core-shell rubber was characterized by transmission electron microscopy. Correlation of the cavitation behaviour at five locations in the stress-whitened zone with the local stress and strain history led to the following conclusions.

1. Cavitation of rubber particles initiates some distance ahead of the notch when a mean stress condition is met. Initially, only a fraction of the particles cavitate and these are randomly distributed.

2. Single cavitated particles grow into cavitated domains by cooperative cavitation of nearby particles. Growth of cavitated domains close to the notch is arrested when shear yielding of the matrix provides an alternative mechanism for relief of strain energy.

3. Cavitated domains far from the notch where the stress state approaches uniaxial tension grow into linear arrays of cavitated particles. Cooperative cavitation of nearby particles may occur by impingement

of a small plastic zone that forms at the equator of a cavitated particle.

Acknowledgements

This research was generously supported by EniChem America Inc. and the National Science Foundation, I/UCRC Program, Grant EEC-9320055.

References

1. C. CHENG, A. HILTNER, E. BAER, P. R. SOSKEY and S. G. MYLONAKIS, *Polymer*, submitted.
2. H.-J. SUE, *J. Mater. Sci.* **27** (1992) 3098.
3. H.-J. SUE, E. I. GARCIA-MEITIN and N. A. ORCHARD, *J. Polym. Sci. B Polym. Phys.* **31** (1993) 595.
4. C. CHENG, A. HILTNER, E. BAER, P. R. SOSKEY and S. G. MYLONAKIS, *J. Appl. Polym. Sci.* **52** (1994) 177.
5. D. HADERSKI, K. SUNG, J. IM, A. HILTNER and E. BAER, *ibid.* **52** (1994) 121.
6. K. SUNG, D. HADERSKI, A. HILTNER and E. BAER, *ibid.* **52** (1994) 147.
7. A. TSE, E. SHIN, A. HILTNER and E. BAER, *J. Mater. Sci.* **26** (1991) 5374.
8. R. HILL, "The Mathematical Theory of Plasticity" (Clarendon, Oxford, 1950).
9. C. CHENG, N. PEDUTO, A. HILTNER, E. BAER, P. R. SOSKEY and S. G. MYLONAKIS, *J. Appl. Polym. Sci.* **53** (1994) 513.
10. A. LAZZERI and C. B. BUCKNALL, *J. Mater. Sci.* **28** (1993) 6799.
11. S. WU, *Polymer* **26** (1985) 1855.

Received 3 June
and accepted 28 June 1994